Crystal and magnetic structures of $Cr_{1/3}NbSe_2$ from neutron diffraction

A. F. Gubkin,[1,2,a)] E. P. Proskurina,[2] Y. Kousaka,[3,4] E. M. Sherokalova,[2] N. V. Selezneva,[2] P. Miao,[5] S. Lee,[5] J. Zhang,[5,6] Y. Ishikawa,[5] S. Torii,[5] T. Kamiyama,[5,7] J. Campo,[8] J. Akimitsu,[3,4] and N. V. Baranov[1,2]

[1]*M.N. Miheev Institute of Metal Physics, Russian Academy of Sciences, 620990 Yekaterinburg, Russia*
[2]*Institute of Natural Sciences, Ural Federal University, 620083 Yekaterinburg, Russia*
[3]*Graduate School of Science, Hiroshima University, Higashi-Hiroshima, Hiroshima 739-8526, Japan*
[4]*Center for Chiral Science, Hiroshima University, Higashi-Hiroshima, Hiroshima 739-8526, Japan*
[5]*Institute of Materials Structure Science, KEK, Tokai, Ibaragi 319-1106, Japan*
[6]*China Spallation Neutron Source, Institute of High Energy Physics, Chinese Academy of Sciences, Dongguan 523803, Guangdong, China*
[7]*Sokendai (Graduate University for Advanced Studies), KEK, Tokai, Ibaragi 319-1106, Japan*
[8]*Aragón Materials Science Institute (CSIC - University of Zaragoza), 50009 Zaragoza, Spain*

(Received 6 October 2015; accepted 23 December 2015; published online 7 January 2016)

Neutron diffraction measurements of the Cr intercalated niobium diselenide $Cr_{1/3}NbSe_2$ together with magnetization measurements have revealed that this compound exhibits ferromagnetic ordering below $T_C = 96$ K unlike a chiral helimagnetic order observed in the sulfide compound $Cr_{1/3}NbS_2$. As derived from neutron diffraction data, the Cr magnetic moments $\mu_{Cr} = 2.83 \pm 0.03\ \mu_B$ in $Cr_{1/3}NbSe_2$ are aligned within basal plane. The discrepancy in the magnetic states of $Cr_{1/3}NbS_2$ and $Cr_{1/3}NbSe_2$ is ascribed to the difference in the preferential site occupation of Cr ions in crystal lattices. In $Cr_{1/3}NbSe_2$, the Cr ions are predominantly distributed over 2*b* Wyckoff site, which determines a centrosymmetric character of the crystal structure unlike $Cr_{1/3}NbS_2$, where the Cr ions are mainly located in 2*c* position and the crystal structure is non-centrosymmetric. © *2016 AIP Publishing LLC*. [http://dx.doi.org/10.1063/1.4939558]

I. INTRODUCTION

Transition metal dichalcogenides TX_2 (T – 3d(4d) transition metal, X = S, Se, or Te) possess a quasi-two dimensional structure where transition metal layer is confined between two chalcogen layers forming a sandwich-like structure. In this structure, the strong covalent bonding within X-T-X tri-layers coexists with the weak van der Waals (vdW) coupling between sandwiches, which allows different atoms to be intercalated into the vdW gap. An intercalation may give rise to dramatic change of the physical properties of parent compounds.[1–4] Among the others, the M_xTX_2 compounds with intercalated magnetoactive M atoms are of particular interest since they represent an analog of artificial multi-layer structures where the M layers are separated by non-magnetic layers. These compounds exhibit a rich variety of magnetic states ranging from spin-glass-like states at low M concentration ($x < 0.25$) up to three dimensional long-range magnetic order at high intercalant concentrations ($x > 0.25$).[5–9] The magnetic properties of these compounds are controlled by combination of reduced dimensionality, ordering effects of intercalated M atoms, magnetocrystalline anisotropy, and exchange interactions of different types. However, not only the type and concentration of inserted M atoms but also non-magnetic TX_2 matrices affect the magnetic order in M_xTX_2. For instance, the transition from the quadruplicated to doubled magnetic unit cell along the *a* and *c* crystallographic axes with the selenium for sulfur substitution in the $Fe_{0.5}TiS_{2-y}Se_y$ compounds was recently reported.[10] The presence of different magnetic states has been revealed in the Cr intercalated compounds $Cr_{0.5}TiSe_2$ and $Cr_{0.5}TiTe_2$ which exhibit incommensurate AFM structure and FM ordering, respectively.[11,12]

Another intriguing example is the $Cr_{1/3}NbS_2$ and $Cr_{1/3}NbSe_2$ compounds, which were reported to exhibit different magnetic states below their critical temperatures. A helimagnetic ground state with a period of about 480 Å was reported for $Cr_{1/3}NbS_2$[13] while the simple ferromagnetic ordering was suggested in $Cr_{1/3}NbSe_2$.[14,15] It should be noted that the $Cr_{1/3}NbS_2$ compound attracts great attention since the application of small magnetic fields results in formation of a chiral soliton lattice with controllable parameters, which opens new possibilities for application in spintronic devices.[16,17] The helimagnetic structure in $Cr_{1/3}NbS_2$ is believed to originate from the Dzyaloshinskii–Moriya (DM) interaction that plays a crucial role in magnetism of non-centrosymmetric compounds with chiral crystal structures.[18,19] Strong coupling between structural and magnetic subsystems in $Cr_{1/3}NbS_2$ has been revealed by x-ray diffraction measurements on the $Cr_{1/3}NbS_2$ powder sample with application of the hydrostatic pressure up to 6.8 GPa.[20] A precise investigation of the crystal structure and magnetic characterization of disordered form of the $Cr_{1/3}NbS_2$ single crystal revealed that Cr atoms disorder substantially affects magnetic ordering temperature as well as the magnetic ground state.[21] The role of structural factors in the formation of chiral magnetic soliton lattice in the intercalation compound $Cr_{1/3}NbS_2$ has been emphasized by means of phenomenological calculations.[22]

Despite the much interest to $Cr_{1/3}NbS_2$ there is a lack of published data on the crystal structure of the $Cr_{1/3}NbSe_2$

a)Author to whom correspondence should be addressed. Electronic mail: agubkin@imp.uran.ru

compound. In accordance with Ref. 23 intercalation of Cr into the niobium diselenide 2*H*-$NbSe_2$ up to $x \approx 1/4$ results in the formation of the $2a_0 \times 2a_0 \times 2c_0$ superstructure, where a_0 and c_0 refer to the primitive hexagonal unit cell of the NiAs structure. At higher intercalant concentration $x = 1/3$ the superstructure type $\sqrt{3}a_0 \times \sqrt{3}a_0 \times 2c_0$ was reported.[14] It has been shown in Refs. 24 and 25 that $\sqrt{3}a_0$-type superstructure in the $M_{1/3}NbS_2$ (M = Cr, Mn, Fe, Co, Ni, or V) compounds can be described with the chiral space group $P6_322$ where intercalated atoms may partially occupy 2*c*, 2*b*, or 2*d* Wyckoff positions. However, to our best knowledge there is neither detailed research of the $Cr_{1/3}NbSe_2$ crystal structure nor magnetic structure characterization. In the present work we performed AC and DC magnetic measurements as well as high resolution neutron powder diffraction (NPD) above and below magnetic ordering temperature in order to revisit the crystal structure and reexamine the magnetic structure of $Cr_{1/3}NbSe_2$.

II. EXPERIMENTAL DETAILS

The polycrystalline sample of $Cr_{1/3}NbSe_2$ was synthesized by means of the one-stage solid state reaction method. The starting materials were Cr powder (purity 99.99%), Nb powder (purity 99.99%), and Se granules (purity 99.99%). The powderized mixture of starting materials was pressed in pellets and put in evacuated quartz ampoules. In total, we prepared 7 ampoules with 1.8 gram pellet-like samples. All the samples were subjected to the identical three-stages heat treatment procedure which includes (i) slowly heating up to $T = 1000\,^{\circ}C$ with the rate of 16.5 °C/h in a furnace, (ii) then the samples were kept for 48 h at 1000 °C and (iii) slowly cooled down to the room temperature with the rate of 196 °C/h. All the synthesized samples were examined using a powder x-ray diffractometer (Bruker D8 ADVANCE) with Cu Kα radiation. A small amount, 2 wt. %, of MO_2 (M = Cr, Nb) impurity phase (rutile-type structure SG $P4_2/mnm$) has been observed on the x-ray diffraction data. AC and DC magnetic measurements were performed by means of a Quantum Design SQUID MPMS magnetometer. The NPD measurements were performed at $T = 10$ K and 132 K using SuperHRPD instrument[26] at the Japan Proton Accelerator Research Complex (J-PARC). Refinement of the crystal structure has been done by means of the Fullprof program.[27]

III. RESULTS AND DISCUSSION

A. Magnetic measurements

The temperature dependencies of the DC magnetic susceptibility for $Cr_{1/3}NbSe_2$ measured using zero field cooling (ZFC) and field cooling (FC) procedures in applied magnetic field of 10 kOe are shown in Figure 1. A drastic rise of the susceptibility below $T_C \approx 100$ K for both curves can be associated with the onset of long-range ferromagnetic order. A slight thermomagnetic hysteresis was observed on the $\chi^{ZFC}(T)$ and $\chi^{FC}(T)$ curves around 95 K. The effective magnetic moment μ_{eff} and paramagnetic Curie temperature θ_p were obtained from a fit of the inverse susceptibility using generalized Curie-Weiss law $\chi = \chi_0 + C/(T - \theta_p)$, where *C* is the Curie constant and χ_0 is the temperature independent

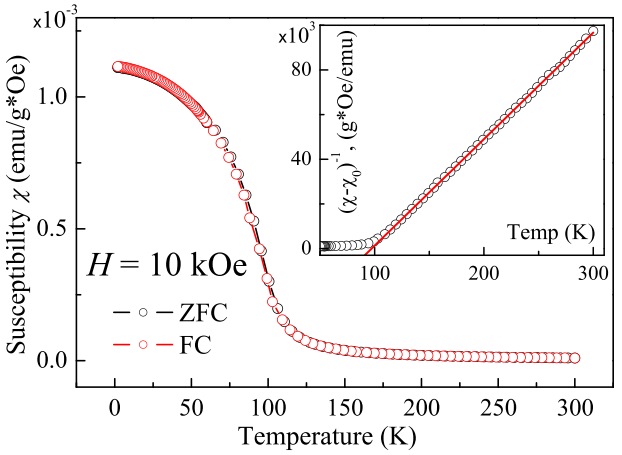

FIG. 1. DC magnetic susceptibility measured using ZFC and FC protocols for $Cr_{1/3}NbSe_2$ polycrystalline sample. The inverse susceptibility $\chi^{-1}(T)$ fitted by the generalised CW law is shown in the inset.

contribution to susceptibility from the Pauli paramagnetism and diamagnetism of the completely filled electronic shells of ions. As one can see from the inset in Figure 1 the inverse susceptibility curve $\chi^{-1}(T)$ well obeys the Curie-Weiss law exhibiting slight upturn below 120 K. The paramagnetic Curie temperature was found to be positive $\theta_p = 97.2$ K, which is in a perfect agreement with the previously reported data $\theta_p = 98$ K[14] and indicates dominance of ferromagnetic exchange interactions. The effective magnetic moment was estimated to be $\mu_{eff} = 3.69\,\mu_B$. This value is in reasonable agreement with the previously reported data for $Cr_{1/3}NbS_2$[13] and the theoretical value for high spin state Cr^{3+} ion $\mu_{eff}^{Cr^{3+}} = 3.87\,\mu_B$. The fitted value of the temperature independent contribution is $\chi_0 = 4 \times 10^{-8}$ emu/g*Oe.

The measurements of the AC magnetic susceptibility were carried out using a driven field amplitude $H_a = 4$ Oe and a frequency $f = \omega/2\pi = 78$ Hz. The temperature dependencies of the in-phase $\chi'(T)$ and out-of-phase $\chi''(T)$ components are shown in Figures 2(a) and 2(b). Here one can observe a step-like rise of the in-phase component at $T_C \approx 96.5$ K. A sharp rise of the $\chi'(T)$ curve is followed by a cusp-like anomaly of the out-of-phase component $\chi''(T)$ around $T_C \approx 96.5$ K. Moreover, out-of-phase component exhibits nearly zero value above and below 96.5 K. Such behavior implies absence of hysteresis losses within the whole temperature range 2–300 K excepting narrow temperature region around T_C which can be ascribed to the onset of long range ferromagnetic order and soft-ferromagnetic behavior below Curie temperature $T_C \approx 96.5$ K

Magnetization isotherm as a function of the applied magnetic field at $T = 2$ K is shown in Figure 3. As one can see, magnetization changes relatively faster in the field range -500 Oe $< H <$ 500 Oe followed by smooth increase in the field range 500 Oe $< H <$ 40 kOe and almost reach a saturation at $H >$ 40 kOe. Such behavior is typical for ferromagnetic systems with strong easy-plane anisotropy. The saturation magnetic moment obtained from the magnetization curve at $H = 50$ kOe was estimated to be $\mu_S^{Cr} = 2.3\,\mu_B$, which is substantially lesser than the theoretical value $3\,\mu_B$ for high spin state Cr^{3+} ion.

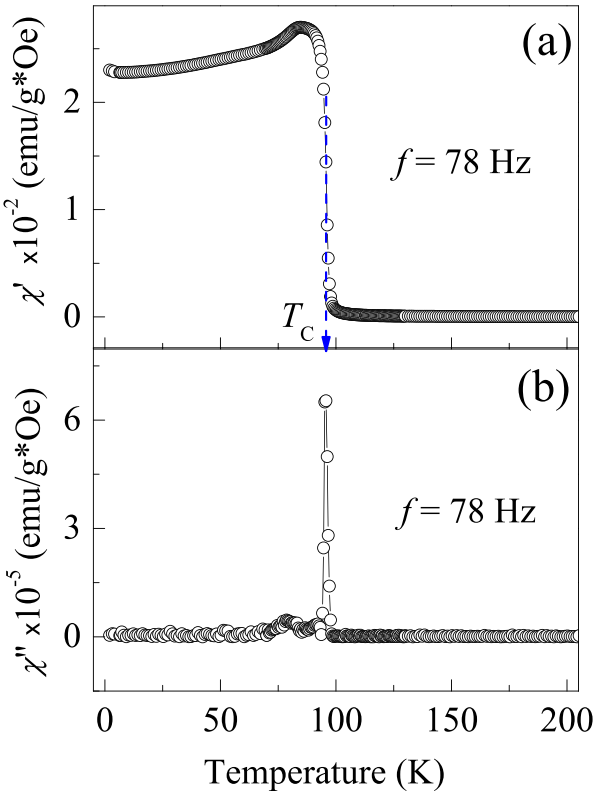

FIG. 2. Temperature dependence of the AC magnetic susceptibility measured for $Cr_{1/3}NbSe_2$ polycrystalline sample: (a) in-phase component $\chi'(T)$ and (b) out-of-phase component $\chi''(T)$.

B. Neutron diffraction above Curie temperature

A high resolution neutron powder diffraction experiment at $T = 132$ K has been performed in order to clarify the crystal structure of $Cr_{1/3}NbSe_2$. It has been found that the measured neutron diffraction pattern can be well indexed by the conventional $\sqrt{3}a_0 \times \sqrt{3}a_0$ superstructure reported for various $M_{1/3}NbX_2$ (X = S, Se) compounds.[23] In accordance with Refs. 24 and 25 such a structure can be described with the space group $P6_322$ and suggests that M atoms predominantly occupy 2*c* (1/3 2/3 1/4) Wyckoff site, while another two accessible positions 2*a* (0 0 0) and 2*b* (2/3 1/3 1/4) are slightly

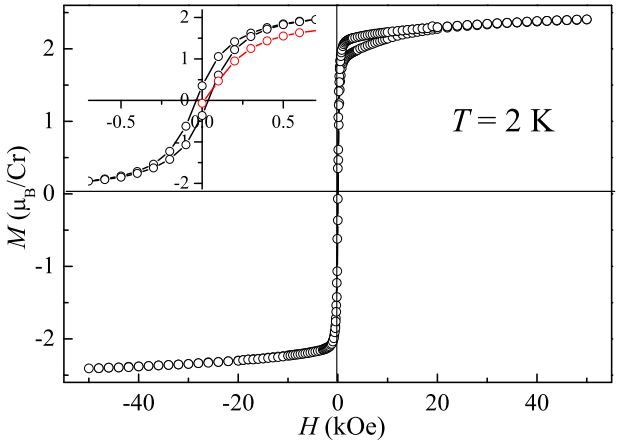

FIG. 3. Field dependence of the magnetization measured at $T = 2$ K for $Cr_{1/3}NbSe_2$ polycrystalline sample. Enlarged part of the hysteresis loop around zero field is shown in the inset.

populated. Later neutron diffraction study of the $Cr_{1/3}NbS_2$ powder sample revealed that Cr atoms occupy 2*c* Wyckoff site with factor 100%.[13] This crystal structure model has been taken as a trial model I for the Rietveld refinement of the neutron diffraction data measured at $T = 132$ K on $Cr_{1/3}NbSe_2$. As one can see from Figure 4(a) and Table I the Rietveld refinement gives obvious discrepancy between observed and calculated profiles for low Q region and relatively high agreement factors. The difference Fourier map

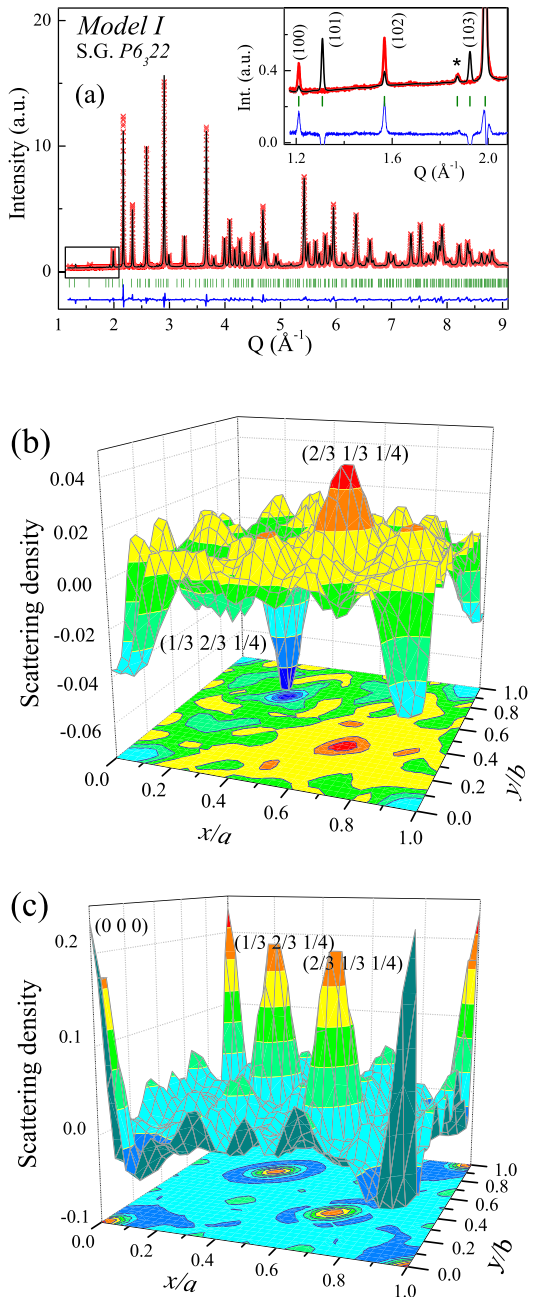

FIG. 4. (a) The best fit result for model I performed on the NPD pattern measured at $T = 132$ K for $Cr_{1/3}NbSe_2$ (see the text). Red symbols are experimental values of the intensity, and black solid line represents the result of the fit. The difference between calculated and observed intensities is shown at the bottom as a solid blue line. The row of green vertical marks below the patterns refers to the nuclear Bragg peaks. Bragg peak (110) given by the impurity phase marked by an asterisk in the inset. The difference Fourier map constructions in the $z/c = 0.25$ plane for model I with fully occupied 2*c* Wyckoff site—(b) and without Cr atoms—(c).

TABLE I. Structural parameters of $Cr_{1/3}NbSe_2$ refined from the neutron diffraction data measured at $T = 132$ K using three models of the crystal structure (see the text). Conventional Rietveld R-factors corrected for background are given at the bottom.

	Model I	Model II	Model III
SG	$P6_322$	$P6_322$	$P6_3/mcm$
Atomic coordinates	$z(Nb) = 0.0008(2)$	$z(Nb) = -0.0017(6)$	$x(Se) = 0.6626(2)$
	$x(Se) = 0.3309(4)$	$x(Se) = 0.3352(4)$	$z(Se) = 0.3821(1)$
	$y(Se) = 0.0034(3)$	$y(Se) = -0.0036(5)$	
	$z(Se) = 0.3678(1)$	$z(Se) = 0.3680(1)$	
Cr occupancy	$Cr^{2c} - 1$	$Cr^{2b} - 0.89(1)$	$Cr^{2b} - 0.90(1)$
	(fixed)	$Cr^{2c} - 0.05(2)$	
		$Cr^{2d} - 0.00(3)$	
Refined stoichiometry	$Cr_{0.33}NbSe_2$	$Cr_{0.31}NbSe_2$	$Cr_{0.30}NbSe_2$
Agreement factors	$\chi^2 = 84.7$, $R_B = 5.2\%$	$\chi^2 = 54.3$, $R_B = 2.5\%$	$\chi^2 = 54.8$, $R_B = 2.2\%$
	$R_{wp} = 11\%$, $R_{exp} = 1.2\%$	$R_{wp} = 8.8\%$, $R_{exp} = 1.2\%$	$R_{wp} = 8.8\%$, $R_{exp} = 1.2\%$

constructed for this model in the $z/c = 0.25$ plane is shown in Figure 4(b). Excess of scattering density manifests itself in the Wyckoff position 2*c* (1/3 2/3 1/4) as a negative peak, while the lack of scattering density can be seen in the Wyckoff position 2*d* (2/3 1/3 1/4) as a positive peak. If all Cr atoms from the cation layer are removed and the difference Fourier map in the $z/c = 0.25$ plane is generated one can observe a pretty symmetric profile with lack of scattering density for 2*b* (0 0 0), 2*c* (1/3 2/3 1/4), and 2*d* (2/3 1/3 1/4) Wyckoff positions (see Figure 4(c)).

Bearing in mind the results of difference Fourier map construction the second crystal structure model (model II) with Cr atoms allowed to be distributed over 2*b*, 2*c*, and 2*d* Wyckoff sites of the $P6_322$ space group was tested by the Rietveld refinement. The unit cell parameters, atomic coordinates, Cr occupancy, and profile function parameters were allowed to be fitted. Despite the good enough agreement factors we were not able to reach convergence on the refinement of model II. Moreover, one can see that low intensity (*h*0*l*) reflections with odd *l* are absent on the experimental pattern, though they exist in model II calculated profile (see Figure 5(a)). Our analysis revealed a predominant occupancy of the 2*b* Wyckoff site with factor 89%, while the occupation factors for both 2*c* ($f \sim 5\%$) and 2*d* ($f \sim 0\%$) sites were found to be comparable with the standard deviations (see Table I). Removal of the 2*c* and 2*d* Wyckoff sites from the model does not substantially affect the goodness of fit and agreement factors. However, one cannot completely exclude a slight occupancy of the 2*c* and 2*d* Wyckoff sites. It should be noted that occupational disorder of Cr atoms was recently observed by x-ray elastic and inelastic scattering on the single crystal sample of $Cr_{1/3}NbS_2$[21] and seems to be an inherent feature of all $M_{1/3}NbX_2$ (X = S or Se) intercalated compounds. Such disorder of intercalant atoms over positions in cation layers strongly depends on the synthesis method and heat treatment protocol.[9,28] However, contrary to the result of our refinement for $Cr_{1/3}NbSe_2$ all the crystal structure studies for $M_{1/3}NbX_2$ reported predominant occupation of the 2*c* Wyckoff site by M atoms.[13,21,24,25]

Detailed inspection of the refined atomic coordinates obtained for model II makes us doubt that the crystal structure of $Cr_{1/3}NbSe_2$ is truly non-centrosymmetric. Indeed in accordance with Ref. 20 distorted CrS_6 octahedra, observed

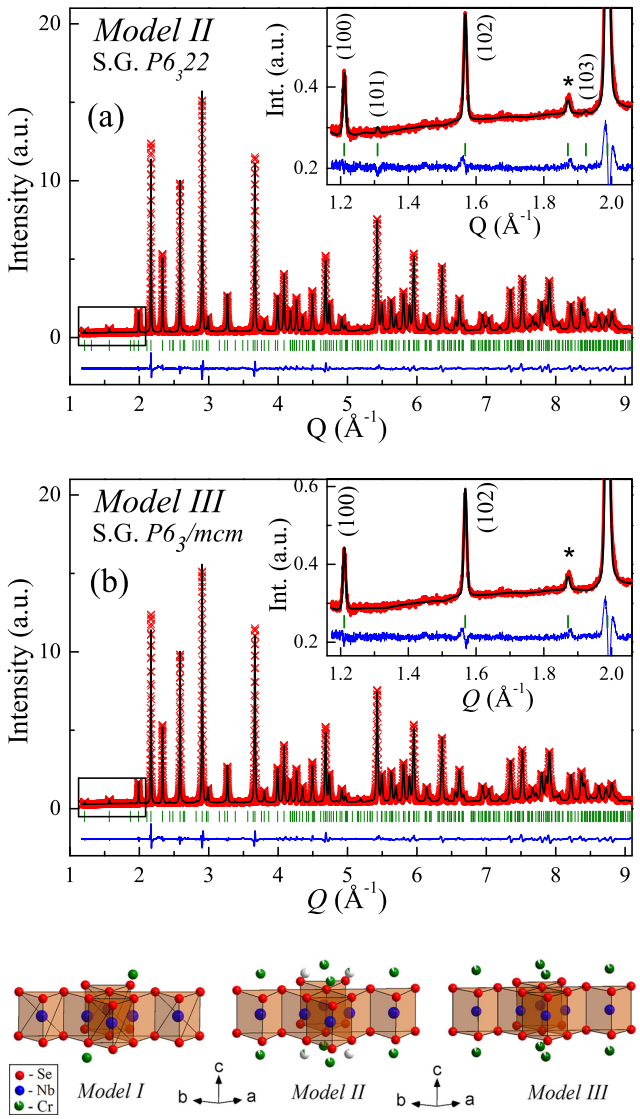

FIG. 5. (a) The best fit result on the NPD pattern for $Cr_{1/3}NbSe_2$ with model II and (b) with model III. Red symbols are experimental values of the intensity, and black solid line represents the result of the fit. The difference between calculated and observed intensities is shown at the bottom as a solid blue line. The row of green vertical marks below the patterns refers to the nuclear Bragg peaks. Bragg peak (110) given by the impurity phase marked by asterisk in the inset. (c) Visualization of the $Cr_{1/3}NbSe_2$ crystal structure refined using models I, II, and III.

in the non-centrosymmetric $Cr_{1/3}NbS_2$, tend to be lesser distorted on application of the hydrostatic pressure up to 6.8 GPa. In $Cr_{1/3}NbSe_2$, $CrSe_6$ octahedra at 2*b*, 2*c*, and 2*d* positions turn out to be almost ideal at normal pressure. In order to check missed symmetry elements the ADDSYM procedure implemented in the PLATON program[29] has been applied to the refined crystal structure with default tolerance parameters. It has been found that ignoring slightly populated 2*c* and 2*d* sites the considered crystal structure possesses missed inversion center and can be described by the space group $P6_3/mcm$ with the origin shifted by (0, 0, −0.25). This new crystal structure model (model III), which suggests that Cr atoms occupy only 2*b* (0 0 0) Wyckoff site of the space group $P6_3/mcm$, has been tested by the Rietveld refinement. The unit cell parameters, atomic coordinates for Se, Cr occupation factor, and profile function parameters were allowed to be refined. As one can see from Figure 5(b), model III shows nice agreement between observed and calculated profiles. We were able to reach convergence on the refinement with the best agreement factors. The refined structural parameters as well as the conventional Rietveld R-factors are represented in Table I. The schematic visualization of the $Cr_{1/3}NbSe_2$ refined crystal structure for all the tested models is shown in Figure 5(c).

A brief comment should be given to the enhanced χ^2 value obtained for all the refined models. An additional Le Bail fit,[30] where peak intensities are optimized without the constraint of a structural model, was performed for the neutron diffraction pattern obtained at 132 K. The conventional Rietveld R-factors were calculated to be $R_{wp} = 8.5\%$, $R_{exp} = 1.2\%$, and $\chi^2 = 50.3$. As one can see these values are as good as the ones obtained from the Rietveld refinement, which indicates that the crystal structure model can no longer be improved.[31] It can be concluded that the enhanced χ^2 values originate from high counting statistics and low experimental uncertainties of the neutron diffraction data.

C. Neutron diffraction below Curie temperature

The magnetic structure of $Cr_{1/3}NbSe_2$ has been studied using low temperature neutron diffraction data measured by both QA and BS detectors of the SuperHRPD instrument. As is shown in Figure 6, an additional contribution to the nuclear Bragg reflections can be observed at the NPD pattern measured at $T = 10$ K. This contribution can be ascribed to the neutron scattering on ferromagnetically ordered Cr spins in $Cr_{1/3}NbSe_2$. However, such contribution may also result from scattering on the long period helicoidal magnetic structure with the propagation vector short enough not being resolved by the instrument. In order to clarify this question we analyzed the profile of the (1 0 2) Bragg peak measured at $T = 132$ K and $T = 10$ K using BS bank which provides the best possible resolution for SuperHRPD. As one can see from the inset in Figure 6 no visible sign of the magnetic satellites typical for helicoidal magnetic structures can be found around (1 0 2) Bragg node at $T = 10$ K. An estimation of the FWHM parameter revealed its increase of about 11% on cooling sample down to 10 K. If one assumes that such increase of the FWHM is due to the magnetic satellite peaks

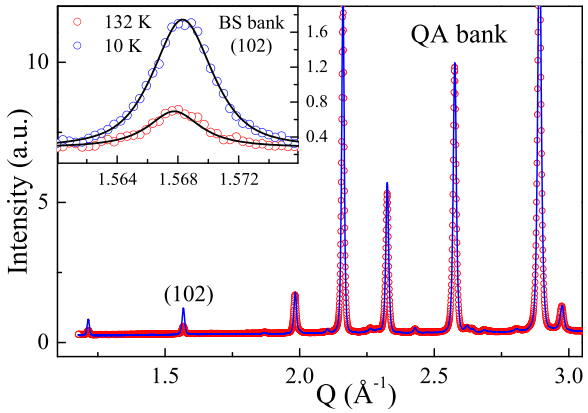

FIG. 6. Neutron diffraction patterns measured by QA-bank at $T = 10$ K (line) and 132 K (circles). Zoomed (1 0 2) Bragg peaks measured by BS-bank at $T = 10$ K and 132 K are shown in the inset.

then the helix period should be over 3000 Å in the real space. Bearing in mind that the crystal structure of $Cr_{1/3}NbSe_2$ is not chiral and exhibits centrosymmetric character with an inversion center between two neighboring Cr atoms along *c*-axis, one can ignore the Dzyaloshinsky-Moriya interaction which plays a key role in formation of the helical magnetic order in the non-centrosymmetric $Cr_{1/3}NbS_2$.[13] The Rietveld refinement of the low temperature $T = 10$ K neutron diffraction pattern revealed that the best fit result ($R_M = 4.5\%$) was obtained for the simple ferromagnetic structure with magnetic moments aligned within the basal plane of the hexagonal unit cell. The refined value of Cr magnetic moment was obtained to be $\mu^{Cr} = 2.83 \pm 0.03\mu_B$.

IV. SUMMARY AND CONCLUSION

In the present work, the crystal structure and magnetic properties of $Cr_{1/3}NbSe_2$ were studied by high resolution powder neutron diffraction, AC and DC magnetic measurements. Three different models of the crystal structure for $Cr_{1/3}NbSe_2$ have been tested by the Rietveld refinement. It has been found that the non-centrosymmetric model II (SG $P6_322$) gives nearly the same agreement factors as the centrosymmetric model III (SG $P6_3/mcm$); nevertheless, bearing in mind the results of the crystal structure analysis performed with the ADDSYM procedure one can suggest that model III is the best one to describe of the $Cr_{1/3}NbSe_2$ crystal structure. The unconstrained refinement of the Cr occupation factors results in $Cr_{0.31}NbSe_2$ stoichiometry for model II and $Cr_{0.30}NbSe_2$ stoichiometry for model III. This result implies that disorder in Cr subsystem and small nonequality in occupancy of the 2*c* and 2*d* Wyckoff sites (model II) cannot be completely excluded. Contrary to the previous works on $M_{1/3}NbX_2$,[13,21,24,25] we found that in $Cr_{1/3}NbSe_2$, Cr atoms are predominantly distributed over 2*b* Wyckoff site. Such a discrepancy may be associated with enhanced covalency of the Se bonds formed with Cr in comparison with the Cr-S bonds in $Cr_{1/3}NbS_2$.

Taking into account the centrosymmetric character of the crystal structure and absence of the contribution from DM interaction one could expect a simple ferromagnetic state emerges on cooling below the Curie temperature in

$Cr_{1/3}NbSe_2$. The results of our AC and DC magnetic measurements proved this suggestion and showed that magnetic state of $Cr_{1/3}NbSe_2$ is a simple ferromagnet. It well agrees with ferromagnetic structure model obtained from the Rietveld refinement of the neutron diffraction data measured at low temperature. However, the detailed DC and AC magnetization measurements on a single crystalline sample of $Cr_{1/3}NbSe_2$ are desirable to support the results of the present work.

ACKNOWLEDGMENTS

This work is partly based on experiments performed at the Japan Proton Accelerator Research Complex J-PARC. This work was performed within the state assignment of the FASO of Russia (No. 01201463334) and supported by Act 211 Government of the Russian Federation (Contract No. 02.A03.21.0006), by the Russian Foundation for Basic Research (Project Nos. 13-02-00364 and 13-02-92104), by the program of UB of RAS (Project No. 15-17-2-22), and by Grants-in-Aid for Scientific Research (Nos. 25220803, 242440590, and 25246006) from the Ministry of Education, Culture, Sports, Science and Technology (MEXT), Japan. This work was also supported by the Center for Chiral Science in Hiroshima University (the MEXT program for promoting the enhancement of research universities, Japan) and JSPS Core-to-Core Program, A. Advanced Research Networks. J.C. and Y.K. acknowledge the Grant No. MAT2011-27233-C02-02.

[1]A. Yoffe, Solid State Ionics **9**, 59 (1983).
[2]M. Inoue, H. Hughes, and A. Yoffe, Adv. Phys. **38**, 565 (1989).
[3]E. Morosan, H. W. Zandbergen, B. S. Dennis, J. W. G. Bos, Y. Onose, T. Klimczuk, A. P. Ramirez, N. P. Ong, and R. J. Cava, Nat. Phys. **2**, 544 (2006).
[4]S. J. Hillenius and R. V. Coleman, Phys. Rev. B **20**, 4569 (1979).
[5]N. Baranov, N. Selezneva, V. G. Pleshchev, N. Mushnikov, and V. Maksimov, Solid State Phenom. **168–169**, 157 (2010).
[6]V. Pleschov, N. Baranov, A. Titov, K. Inoue, M. Bartashevich, and T. Goto, J. Alloys Compd. **320**, 13 (2001).
[7]H. Negishi, A. Shoube, H. Takahashi, Y. Ueda, M. Sasaki, and M. Inoue, J. Magn. Magn. Mater. **67**, 179 (1987).
[8]S. S. P. Parkin and R. H. Friend, Philos. Mag. B **41**, 65 (1980).
[9]N. V. Baranov, E. M. Sherokalova, N. V. Selezneva, A. V. Proshkin, A. F. Gubkin, L. Keller, A. S. Volegov, and E. P. Proskurina, J. Phys.: Condens. Matter **25**, 066004 (2013).
[10]A. Gubkin, E. Sherokalova, L. Keller, N. Selezneva, A. Proshkin, E. Proskurina, and N. Baranov, J. Alloys Compd. **616**, 148 (2014).
[11]N. V. Baranov, A. N. Titov, V. I. Maksimov, N. V. Toporova, A. Daoud-Aladine, and A. Podlesnyak, J. Phys.: Condens. Matter **17**, 5255 (2005).
[12]N. V. Baranov, V. G. Pleshchev, N. V. Selezneva, E. M. Sherokalova, A. V. Korolev, V. A. Kazantsev, and A. V. Proshkin, J. Phys.: Condens. Matter **21**, 506002 (2009).
[13]T. Miyadai, K. Kikuchi, H. Kondo, S. Sakka, M. Arai, and Y. Ishikawa, J. Phys. Soc. Jpn. **52**, 1394 (1983).
[14]F. Hulliger and E. Pobitschka, J. Solid State Chem. **1**, 117 (1970).
[15]W. Z. Hu, G. T. Wang, R. Hu, C. Petrovic, E. Morosan, R. J. Cava, Z. Fang, and N. L. Wang, Phys. Rev. B **78**, 085120 (2008).
[16]Y. Togawa, T. Koyama, K. Takayanagi, S. Mori, Y. Kousaka, J. Akimitsu, S. Nishihara, K. Inoue, A. S. Ovchinnikov, and J. Kishine, Phys. Rev. Lett. **108**, 107202 (2012).
[17]Y. Togawa, Y. Kousaka, S. Nishihara, K. Inoue, J. Akimitsu, A. S. Ovchinnikov, and J. Kishine, Phys. Rev. Lett. **111**, 197204 (2013).
[18]P. Bak and M. H. Jensen, J. Phys. C **13**, L881 (1980).
[19]S. V. Maleyev, Phys. Rev. B **73**, 174402 (2006).
[20]M. Mito, T. Tajiri, K. Tsuruta, H. Deguchi, J. Kishine, K. Inoue, Y. Kousaka, Y. Nakao, and J. Akimitsu, J. Appl. Phys. **117**, 183904 (2015).
[21]V. Dyadkin, F. Mushenok, A. Bosak, D. Menzel, S. Grigoriev, P. Pattison, and D. Chernyshov, Phys. Rev. B **91**, 184205 (2015).
[22]L. M. Volkova and D. V. Marinin, J. Appl. Phys. **116**, 133901 (2014).
[23]J. Voorhoeve, N. van den Berg, and M. Robbins, J. Solid State Chem. **1**, 134 (1970).
[24]J. van den Berg and P. Cossee, Inorg. Chim. Acta **2**, 143 (1968).
[25]B. van Laar, H. Rietveld, and D. Ijdo, J. Solid State Chem. **3**, 154 (1971).
[26]S. Torii, M. Yonemura, T. Y. S. P. Putra, J. Zhang, P. Miao, T. Muroya, R. Tomiyasu, T. Morishima, S. Sato, H. Sagehashi, Y. Noda, and T. Kamiyama, J. Phys. Soc. Jpn. **80**, SB020 (2011).
[27]J. Rodríguez-Carvajal, Physica B **192**, 55 (1993).
[28]V. G. Pleshchev, N. V. Selezneva, V. I. Maksimov, A. V. Korolev, A. V. Podlesnyak, and N. V. Baranov, Phys. Solid State **51**, 933 (2009).
[29]A. L. Spek, Acta Crystallogr., Sect. D **65**, 148 (2009).
[30]A. L. Bail, H. Duroy, and J. Fourquet, Mater. Res. Bull. **23**, 447 (1988).
[31]B. H. Toby, Powder Diffr. **21**, 67 (2006).